

## *t*-Channel Couplings in Kaon-Nucleon Scattering

R.A.W. Bradford and B.R. Martin

Department of Physics and Astronomy, University College London, Gower Street, London WC1E 6BT, U.K.

**Abstract.** Hyperbolic dispersion relations are used to examine elastic  $KN$  and  $\bar{K}N$  amplitudes in the resonance region, and to extrapolate them to the annihilation channel. By evaluating the relations on a set of paths interior to the elastic channel physical regions, a spin separation of  $t$ -channel contributions is effected, and resonance couplings deduced. The results show clear evidence for effects attributable to exchanges with  $J \leq 3$ , several of which have not previously been isolated. The special problems associated with the isoscalar  $S$ -wave states are discussed, and an estimate made of the  $\varepsilon - S^*$  mixing angle.

### 1. Introduction

Dispersion relations, by imposing general constraints from analyticity and crossing symmetry, have been powerful tools for the phenomenological analysis of data on two-body processes, both in the resonance region [1], and at intermediate energies [2]. However, most dispersion relations have drawbacks in practice. For example, in partial-wave relations large regions of the left-hand cuts are usually unknown, and in fixed- $t$  relations substantial extrapolations outside the physical region are required. Such problems are largely absent in dispersion relations where the integrations are performed along hyperbolas in the Mandelstam plane, chosen to avoid passing through double spectral regions. Moreover, by varying the hyperbola parameter, a simple spin separation of  $t$ -channel amplitudes is effected, which is difficult to achieve by other means (e.g. by using backward dispersion relations).

Hyperbolic dispersion relations have been used to study  $t$ -channel couplings in  $\pi N$  scattering [3,4], and have produced new values for the couplings of mesons with  $J \leq 3$ , as well as interesting evidence for states with  $J = 4$  and 5 close to the  $N\bar{N}$  threshold. In this paper we apply similar techniques to the kaon-nucleon system.

This system has a number of additional complications. For example,  $G$ -parity provides no restrictions on the  $t$ -channel, and amplitudes for both strangeness  $S = +1$  ( $KN$ ) and  $-1$  ( $K\bar{N}$ ) channels are needed as input, both of which are subject to more uncertainties than the corresponding  $\pi N$  ones. We have therefore to examine the mutual compatibility of different possible sets of input data before extrapolating a consistent set to the  $t$ -channel to obtain resonance couplings. The results show clear evidence for effects attributable to states with  $J \leq 3$ , several of which have not previously been isolated. The isoscalar  $S$ -wave is particularly interesting and leads to couplings which, together with decay information, enable the  $\varepsilon - S^*$  mixing angle to be estimated.

### 2. Formalism

#### 2.1. Kinematics and Amplitudes

We work with the usual  $KN$  ( $s$ -channel) invariant amplitudes [5]  $A^I$  and  $B^I$  for isospin  $I = 0$  and 1, and in addition the amplitude

$$C \equiv -\frac{1}{4}[4p^2 A - MvB],$$

where  $p^2 = (t/4 - M^2)$ ;  $v \equiv (s - u)$ ;  $M$  is the nucleon mass; and  $s, t$  and  $u$  are the usual Mandelstam invariants. Amplitudes for  $\bar{K}N$  scattering ( $u$ -channel) are denoted by  $\tilde{A}^I, \tilde{B}^I$  and  $\tilde{C}^I$ . Useful isospin combinations are

$$A^+ \equiv \frac{1}{4}[3A^1 + A^0], A^- \equiv \frac{1}{4}[A^1 - A^0],$$

and similarly for  $B, \tilde{A}$  etc. Under  $s \leftrightarrow u$  crossing

$$A^\pm(v, t) \rightarrow \pm \tilde{A}^\pm(-v, t), B^\pm(v, t) \rightarrow \mp \tilde{B}^\pm(-v, t).$$

Amplitudes with definite  $su$  crossing symmetry are defined by

$$F_1^\pm \equiv C^+ \pm \tilde{C}^+, F_2^\pm \equiv C^- \mp \tilde{C}^-, \\ F_3^\pm \equiv B^+ \mp \tilde{B}^+, F_4^\pm \equiv B^- \pm \tilde{B}^-$$

These have the following  $t$ -channel partial-wave

expansions:

$$F_{1,2}^{\pm}(t, z) = 2\pi \sum_J (2J+1) (pq)^J P_J(z) \cdot [1 \pm (-1)^J] h_{\pm}^{J(0,1)}(t), \quad (2.1)$$

$$F_{3,4}^{\pm}(t, z) = 2\pi \sum_J \frac{(2J+1)}{\sqrt{J(J+1)}} (pq)^{J-1} P'_J(z) \cdot [1 \mp (-1)^J] h_{\pm}^{J(0,1)}(t),$$

where  $q^2 = (t/4 - m^2)$ ;  $m$  is the kaon mass;  $z$  is the cosine of the  $t$ -channel scattering angle; and  $h_{\pm}^{J(I)}$  is the  $t$ -channel (taken to be  $\bar{K}K \rightarrow \bar{N}N$ ) partial-wave helicity ( $\pm$ ) amplitude for  $t$ -channel isospin  $I = 0, 1$ . For example, the  $\rho$ -meson contributes to  $F_2^-$  and  $F_4^+$ .

## 2.2. Hyperbolic Dispersion Relations

Dispersion relations may be written for any crossing symmetric amplitude along hyperbolas

$$(s-a)(u-a) = b$$

in the Mandelstam plane [6]. In our case we choose

$$b = [(M+m)^2 - a][(M-m)^2 - a],$$

so that all paths pass through the KN threshold  $s = (M+m)^2, t = 0$ , and lie interior to the elastic channel physical regions, leaving  $a$  as the hyperbola parameter. Other paths are possible [4], but all have the disadvantage of involving unphysical values of the  $s$  and  $u$ -channel scattering angles, which causes an undesirable enhancement at low energies of poorly known higher partial waves.

For the amplitudes  $F_i^{\pm}$ , the unsubtracted dispersion relations take the form

$$F_i^{\pm}\{s, t(a, s)\} = P_i^{\pm} + \frac{v^N}{\pi} \int_{4\mu^2}^{\infty} \text{Im} \left\{ \frac{F_i^{\pm}\{t', s'(a, t')\}}{v'^N} \right\} \frac{dt'}{t' - t} + \frac{1}{\pi} \int_T^{\infty} \text{Im} F_i^{\pm}\{s', t'(a, s')\} \{s', s, a\}^{\pm} ds', \quad (2.2)$$

where  $P_i^{\pm}$  is the contribution of pole terms;  $T = (M_A + \mu)^2$  is the lowest  $u$ -channel threshold;  $\mu \equiv m_{\pi}$ ;  $N = 0$  (1) for  $F_i^+$  ( $F_i^-$ );

$$\{s', s, a\}^+ \equiv \left[ \frac{1}{s' - s} + \frac{1}{s' - u} - \frac{1}{s' - a} \right], \quad (2.3)$$

and

$$\{s', s, a\}^- \equiv \left[ \frac{1}{s' - s} - \frac{1}{s' - u} \right]. \quad (2.4)$$

In the kaon-nucleon case the single-particle terms  $P_i^{\pm}$  are due to the  $\Lambda$  and  $\Sigma$  poles. These Born terms are given by

$$P_{1,2}^{\pm} = \pm \sum_Y C_{1,2}(Y) P_Y G_Y^2 \{M_Y^2, s, a\}^{\pm}$$

and

$$P_{3,4}^{\pm} = \mp \sum_Y C_{3,4}(Y) G_Y^2 \{M_Y^2, s, a\}^{\pm},$$

where the sum is over  $Y = \Lambda, \Sigma$ ;  $G_Y$  is the usual pseudoscalar KNY coupling constant;

$$P_Y \equiv p_Y^2 (M_Y - M) + M v_Y / 4;$$

and the coefficients are given by

$$C_1(\Lambda) = C_2(\Lambda) = C_3(\Lambda) = C_4(\Sigma) = -C_2(\Sigma) \\ = -C_4(\Lambda) = \frac{1}{2}, C_1(\Sigma) = C_3(\Sigma) = \frac{3}{2}.$$

Subscripted quantities are evaluated on the relevant hyperbola at  $s = M_Y^2$ , and are thus functions of  $a$ .

In practice the below-threshold  $\Sigma^*$  state P13 (1385) is also treated in the narrow-width approximation, and so additional contributions which must be added to (2.2) are:

$$P_{1,2}^{\pm}(\Sigma^*) = \pm D_{1,2} P_{\Sigma^*} G_{\Sigma^*}^2 \{M_{\Sigma^*}^2, s, a\}^{\pm},$$

$$P_{3,4}^{\pm}(\Sigma^*) = \mp D_{3,4} (\beta_1 + \beta_2 t_{\Sigma^*}^*) G_{\Sigma^*}^2 \{M_{\Sigma^*}^2, s, a\}^{\pm},$$

where  $D_1 = D_3 = \frac{1}{4}$ ,  $D_2 = D_4 = -\frac{1}{2}$ ;  $G_{\Sigma^*}$  is the  $\text{KN}\Sigma^*$  coupling;  $t_{\Sigma^*}$  is the value of  $t$  such that on the hyperbola defined by  $a, u = M_{\Sigma^*}^2$ ; and the other kinematical quantities are defined as follows:

$$P_{\Sigma^*} = -p_{\Sigma^*}^2 (\alpha_1 + \alpha_2 t_{\Sigma^*}^*) + \frac{M v_{\Sigma^*}}{4} (\beta_1 + \beta_2 t_{\Sigma^*}^*),$$

$$\alpha_1 = 3(M_{\Sigma^*} + M) q_{\Sigma^*}^2 + (M_{\Sigma^*} - M) \left[ \frac{(M_{\Sigma^*} + M)^2 - m^2}{2M_{\Sigma^*}} \right]^2,$$

$$\beta_1 = 3q_{\Sigma^*}^2 - \left[ \frac{(M_{\Sigma^*} + M)^2 - m^2}{2M_{\Sigma^*}} \right]^2,$$

$$\alpha_2 = \frac{3}{2}(M_{\Sigma^*} + m), \quad \beta_2 = \frac{3}{2}.$$

## 3. $t$ -Channel Extrapolations

### 3.1. Kaon-Nucleon Data Input

To extract information on the  $t$ -channel process  $\bar{K}K \rightarrow \bar{N}N$  we first form the "discrepancy" function

$$D_i^{\pm}(t, a) \equiv \text{Re} F_i^{\pm}(s, t) - P_i^{\pm}(s, a) - \frac{P}{\pi} \int_T^{\tilde{s}} \text{Im} F_i^{\pm}(s', t') \{s', s, a\}^{\pm} ds, \quad (3.1)$$

which consists of those parts of the dispersion relations which can be evaluated with currently available  $s$  and  $u$ -channel data.

In the  $s$ -channel we use the amplitudes from Ref [7], which is the latest and most extensive analysis of both KN isospin channels. The upper momentum of this analysis ( $k_{\text{lab}} = 1.5 \text{ GeV}/c$ ) determines the upper limit  $\tilde{s}$ .

The latest analysis of  $u$ -channel data below 1.5 GeV/c is by a Berkeley group [8] (which we denote by BK). This extends to lower momenta than previous analyses, fits new low-momentum  $K^-p$  elastic polarization data, and includes some constraints from forward dispersion relations. Hence it is intrinsically more reliable than earlier work, and we use it as our preferred input in this region. Nevertheless,

for the purpose of comparison, and to estimate errors, we also use the amplitudes of the Rutherford Lab.—Imperial College collaboration [9] (denoted RLIC), and those of the University College group [10] (denoted UCL), which analyze most of the data used by BK. In the case of the UCL solution an explicit resonance form for the D03 (1520) resonance must be added, as the lowest energy of the analysis is 1540 MeV. This is done using a Breit-Wigner formula with a standard Blatt and Weisskopf barrier factor.

The  $u$ -channel amplitudes in the resonance region must be supplemented by amplitudes at very low energies. Here we use the results of the  $K$ -matrix analysis of [11], which is the most reliable available, mainly because of the simultaneous use of data and forward dispersion relations. In particular, consistency was required, via forward dispersion relations, with the forward  $K^-p$  charge-exchange differential cross-section, which had previously been neglected. We analytically continue the  $K$ -matrix amplitudes below the  $\bar{K}N$  threshold to provide a model for the  $\bar{K}N$  unphysical region also.

Another result of the analysis of [11] is a more reliable determination of the  $KN\Lambda$  coupling constant ( $G_{KN\Lambda}^2/4\pi = 13.7 \pm 2.7$ ) which we use to evaluate the  $\Lambda$ -pole term in (2.2). In the case of the  $\Sigma$  it proved difficult to separate its contribution from that of the  $\Sigma^*$ , the best-value ( $G_{\Sigma}^2/4\pi = 3.7$ ) being obtained with the  $\Sigma^*$  coupling essentially zero. Since away from  $t=0$  even a small  $\Sigma^*$  coupling could give rise to important contributions, we also consider the possibility of a non-zero  $\Sigma^*$  coupling,  $G_{\Sigma^*}^2/4\pi = 2.6$  (which is somewhat less than the  $SU(3)$  value), and in this case reduce  $G_{\Sigma}^2$  so that the total contribution of  $\Sigma$  plus  $\Sigma^*$  to the forward amplitude at threshold is conserved, thereby preserving the consistency between the  $K$ -matrix predictions and the forward dispersion relation fits of [11]. The actual value used for  $G_{\Sigma}^2/4\pi$  in this case is 2.5.

### 3.2. Use of Fixed- $t$ Dispersion Relations

Two problems are raised by the use of the above  $u$ -channel input. Firstly, there are discontinuities at the joining momentum between the  $K$ -matrix amplitudes [11] and those from the analyses in the resonance region [8–10]. Although the matching problem is less severe for the BK analysis, which imposed forward dispersion relation constraints [11], even this solution has problems away from  $t=0$ . Part of this trouble could well be due to the fact that the  $K$ -matrix analysis only includes  $S$ -waves. This raises the second problem, that  $\text{Re } \tilde{B}^I$  will be very poorly reconstructed at low momenta because threshold effects enhance  $P$ -waves there.

The practical effect of these problems is to produce an unsmooth behaviour in  $D_i^\pm$ , as calculated from (3.1), as functions of  $t$  (at fixed- $a$ ) for  $-t \lesssim 0.3 \text{ GeV}^2$ ,

which is particularly unfortunate as this region is expected to play an important role in the interpretation of the discrepancies in terms of  $t$ -channel poles.

A solution to this problem is to calculate the real parts appearing in (3.1) from fixed- $t$  dispersion relations, since the  $S$ -wave approximation for the imaginary parts at very low momenta is expected to be adequate. For the amplitudes  $F_i$  the relations have the unsubtracted forms [5],

$$\text{Re } F_i^\pm(s, t) = P_i^\pm(s, t) + \frac{P}{\pi} \int_T^\infty \text{Im } F_i^\pm(s', t) \left[ \frac{1}{s' - s} \pm \frac{1}{s' - u} \right] ds', \quad (3.2)$$

where the fixed- $t$  poles (including the  $\Sigma^*$  (1385)) are given by

$$P_{1,2}^\pm = \pm \left[ \sum_Y C_{1,2}(Y) Q_Y G_Y^2 \langle M_Y \rangle^\pm + D_{1,2} Q_{\Sigma^*} G_{\Sigma^*}^2 \langle M_{\Sigma^*} \rangle^\pm \right],$$

$$P_{3,4}^\pm = \mp \left[ \sum_Y C_{3,4}(Y) G_Y^2 \langle M_Y \rangle^\pm + D_{3,4} (\beta_1 + \beta_2 t) G_{\Sigma^*}^2 \langle M_{\Sigma^*} \rangle^\pm \right],$$

$$\text{where } \langle M \rangle^\pm \equiv \frac{1}{M^2 - s} \pm \frac{1}{M^2 - u}$$

$$Q_Y \equiv -(t/4 - M^2)(M - M_Y) + M(2M_Y^2 + t - \Sigma)/4,$$

$$Q_{\Sigma^*} \equiv -(t/4 - M^2)(\alpha_1 + \alpha_2 t) + M(2M_{\Sigma^*}^2 + t - \Sigma)(\beta_1 + \beta_2 t)/4,$$

and

$$\Sigma \equiv 2(M^2 + m^2).$$

These relations may be evaluated using the input data discussed above, and a model for the small- $t$  high-energy behaviour. For the latter we use the Regge-pole solution of [12].

Although the use of fixed- $t$  relations is strictly necessary only for  $-t \lesssim 0.3 \text{ GeV}^2$ , in practice we use them for the entire  $t$ -range considered to avoid generating further discontinuities. The latter range is  $-t \leq 0.8 \text{ GeV}^2$ , which is slightly larger than allowed by a strict application of Manderlstaam analyticity. Both  $s$ - and  $u$ -channel real parts were calculated in this way, and to ensure convergence of the integrals a subtraction was made at  $\sqrt{s} = 1.75 \text{ GeV}$ , where all three  $u$ -channel phase shift analyses [8–10] are in excellent agreement.

It is, of course, important to check that the predicted real parts are in agreement with those from the phase shift analyses in the physical regions appropriate to each  $t$ -value. In the  $s$ -channel the agreement is satisfactory. In the  $u$ -channel the BK amplitudes have overall the greatest degree of consistency (which

is another reason for using them as our preferred  $u$ -channel input), although  $\text{Re } \tilde{B}^1$  is sensitive to the precise values of the  $\Sigma$  and  $\Sigma^*$  couplings. The RLIC and UCL solutions are also satisfactory, with the exception of  $\text{Re } \tilde{B}^0$  and the UCL case. However, since only the imaginary parts will be explicitly used in the hyperbolic dispersion relations, we retain all three sets of amplitudes.

As a byproduct of the fixed- $t$  analysis we evaluate (3.2) at  $t = 0$  to obtain estimates of the  $\bar{K}NS$  and  $P$ -wave scattering lengths (the notation is  $a_{l\pm}^{(J)}$  corresponding to  $J = l \pm 1/2$ ):

$$\begin{aligned} a_{0+}^{(0)} &= -1.79 \pm 0.16 fm, \\ a_{1-}^{(0)} - a_{1+}^{(0)} &= 0.04 \pm 0.02 fm^3, \\ a_{0+}^{(1)} &= 0.41 \pm 0.07 fm, \\ a_{1-}^{(1)} - a_{1+}^{(1)} &= 0.02 \pm 0.07 fm^3. \end{aligned}$$

The errors arise from using the different inputs described above.

### 3.3. $t$ -Channel Models

From equations (2.2) and (3.1)

$$D_i^\pm(t, a) = v^N H_i^\pm(t, a) + \frac{v^N}{\pi} \int_{4\mu^2}^{\tilde{t}} \text{Im} \left[ \frac{F_i^\pm(t', s')}{v'^N} \right] \frac{dt'}{t' - t}, \quad (3.3)$$

where the function  $H_i^\pm(t, a)$  is the sum of the high-energy parts of the  $s$  and  $u$ -channel integrations above the phase-shift region  $(M + m)^2 \leq s' \leq \tilde{s}$ , and the  $t$ -channel integration above  $t = \tilde{t}$ , which varies with the particular amplitude but is of the order of  $4M^2$ .

Since  $\tilde{t}$  is far from the region of evaluation of  $D_i^\pm(t, a)$  ( $0 \leq -t \leq 0.8 \text{ GeV}^2$ ), we may safely assume that the physical region of the  $t$ -channel gives only a  $t$ -independent contribution to the discrepancy (or a contribution proportional to  $v(t, a)$  in the crossing-odd case). We make the same assumption for the high-energy  $s$  and  $u$ -channel contributions also, although here we are on less sure ground. However, the relevant Regge exchanges are either exotic or exchange—degenerate, so it is likely that the total  $s$ - and  $u$ -channel contribution is very small, in which case this assumption will make negligible error. Since in practice none of the functions  $D_i^\pm$  turns out to have more than one turning point as a function of  $a$  at any fixed value of  $t$ , the simplest model for  $H_i^\pm(a)$  is a quadratic. A more satisfactory procedure is to make a fixed- $a$  subtraction, and hence remove  $H_i^\pm$ . Thus, if the discrepancies are subtracted at  $t = t_2$ , and evaluated at  $t = t_1$ , we work with the quantities.

$$A_i^\pm(t_1, t_2, a) \equiv \frac{D_i^\pm(t_1, a)}{v^N(t_1, a)} - \frac{D_i^\pm(t_2, a)}{v^N(t_2, a)}. \quad (3.4)$$

The subtraction will also improve the convergence

of the integrals. Using the subtracted forms, and the unsubtracted forms with  $H(a)$  a quadratic, produces negligible changes in the  $t$ -channel couplings, which suggests that the effects of distant cuts have been satisfactorily separated from the lower-mass exchanges.

As a model for the latter we evaluate the integral in (3.3) using the partial-wave helicity expansion (2.1) truncated after  $n$  terms, and for each discrepancy we perform fits with  $n = 1, 2$  and  $3$ . Using the relation

$$z = 1 + at/pq,$$

in the Legendre polynomials, gives the  $a$  dependence of the various helicity amplitudes. For each discrepancy the  $n^{\text{th}}$  contributing amplitude in order of increasing spin has an  $a$  dependence given by an  $(n - 1)$ th polynomial. Each helicity amplitude is assumed to be dominated by at most two states, and for each we use the narrow-width approximation, i.e.

$$h_\pm^R(t) = \frac{2\Gamma_\pm^R}{M_R - t - i\varepsilon},$$

where  $R$  denotes the appropriate  $t$ -channel resonance. In the case of the isoscalar  $S$ -wave amplitude, where the states are probably very broad, an alternative to the narrow-width form was used, and this will be discussed in Sect. 4. The masses  $M_R$  were taken to be those of known mesons, or for the higher spin states from an assumed linear Regge trajectory, although in the final solutions only known states were needed to fit the discrepancies. The free parameters are the couplings  $\Gamma_\pm^R$ , and these are determined by simultaneously fitting the discrepancies over the entire grid of  $a$  and  $t$ -values (or the grid of  $a, t_1$ , and  $t_2$  in the case of the subtracted discrepancies). The range of the former,  $-1.8 \text{ GeV}^2 \leq a \leq 0$ , is determined by the convergence of the  $t$ -channel helicity expansion on the hyperbolic paths used, assuming Mandelstam analyticity.

## 4. $t$ -Channel Couplings

### 4.1. $\rho$ and $g$ Mesons

These contribute to the discrepancies  $D_4^+$  and  $D_2^-$ , and in both cases a satisfactory fit is obtained with just the two lowest spin partial-wave helicity amplitudes. In fact the  $\rho$  alone gives quite reasonable fits. However, inclusion of the  $g$ -meson produces a small, but significant, improvement, and the subtracted discrepancies  $A_4^+$  and  $A_2^-$  show some  $a$ -dependence at fixed- $t$ , indicating the presence of an amplitude with  $J > 1$ . Moreover, the various choices of input lead to consistent values for the residues  $\Gamma_\pm^g$ . The fit to  $D_4^+$  and  $D_2^-/v$  using the BK amplitudes as the main  $u$ -channel input, are shown in Fig. 1.

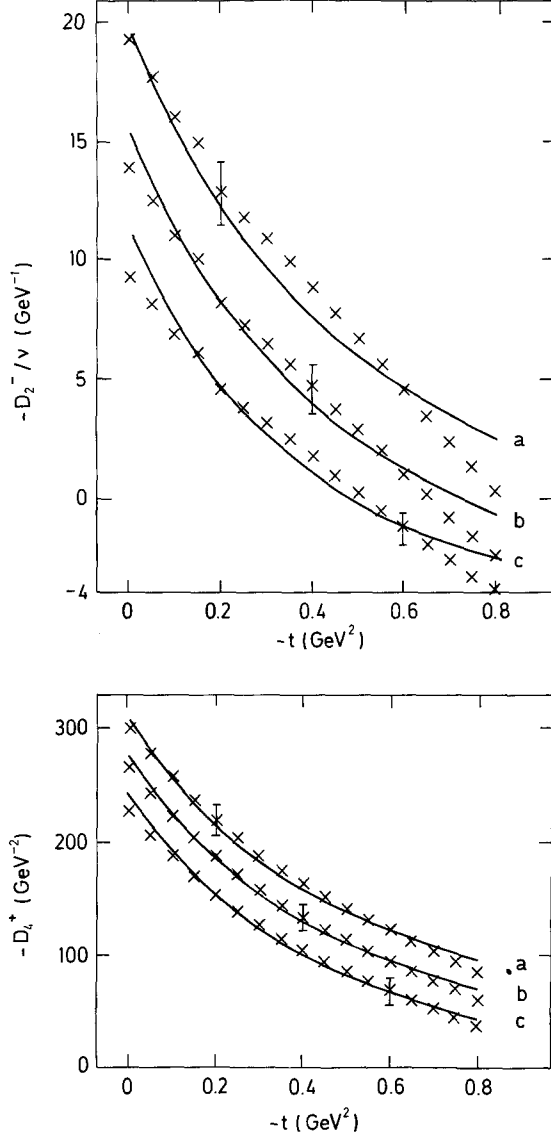


**Fig. 1.** Fit (—), using  $\rho$  and  $g$  contributions, to the  $t$ -dependence of  $D_4^+$  and  $D_2^-/\nu(x)$ , for  $a=0$  (a),  $a=-0.6 \text{ GeV}^2$  (b), and  $a=-1.8 \text{ GeV}^2$  (c). Some typical error bars are shown

The fitted values for the  $\rho$ -residues are

$$\Gamma_+^{\rho} = -0.89 \pm 0.12, \quad \Gamma_-^{\rho} = -4.1 \pm 0.4, \quad (4.1)$$

where the units are appropriate powers of GeV. It is convenient to relate these residues to conventional coupling constants, and since we work in Born approximation this may be done by defining effective Lagrangian densities. For definiteness we use the conventions of [13], which lead to dimensionless coupling constants. The relations are

$$\Gamma_+^{\rho} = -\frac{M}{6} \frac{G_{\rho K\bar{K}}}{4\pi} \left( G_{\rho N\bar{N}}^{(V)} + \frac{m_{\rho}^2}{4M^2} G_{\rho N\bar{N}}^T \right), \quad (4.2)$$

and

$$\Gamma_-^{\rho} = -\frac{\sqrt{2}}{6} \frac{G_{\rho K\bar{K}}}{4\pi} (G_{\rho N\bar{N}}^{(V)} + G_{\rho N\bar{N}}^{(T)}). \quad (4.3)$$

Using (4.1) gives

$$G_{\rho N\bar{N}}^{(T)}/G_{\rho N\bar{N}}^{(V)} = 4.2 \pm 2.4, \quad (4.4)$$

in reasonable agreement with the best estimate from  $\pi N$  analyses [13] ( $6.3 \pm 0.9$ ). The large error on this ratio is due to cancellations in equations (4.2) and (4.3), and so it is probably more reasonable to use the intrinsically more reliable value from  $\pi N$  analyses. We then obtain from (4.2) and (4.3) estimates for  $G_{\rho K\bar{K}} G_{\rho N\bar{N}}^{(V)}/4\pi$ , which when averaged give  $2.6 \pm 0.4$ . Since the best estimate of  $G_{\rho\pi\pi} G_{\rho N\bar{N}}^{(V)}/4\pi$  is  $2.4 \pm 0.4$  [13] we have

$$G_{\rho K\bar{K}}/G_{\rho\pi\pi} = 1.08 \pm 0.35,$$

in excellent agreement with the pure SU(3) prediction of unity, and an application of hyperbolic dispersion relations to  $\pi K$  scattering [14] which finds  $0.95 \pm 0.09$ . (Using (4.4) leads to  $G_{\rho K\bar{K}}/G_{\rho\pi\pi} = 1.4 \pm 0.6$ ).

The fitted values of the  $g$ -residues are

$$\Gamma_+^g = -0.30 \pm 0.14, \quad \Gamma_-^g = -0.35 \pm 0.14. \quad (4.5)$$

These are related to dimensionless coupling constants by

$$\Gamma_+^g = \frac{-128}{35\mu^2 M} \frac{G_{gK\bar{K}}}{4\pi} \left( G_{gN\bar{N}}^{(1)} - \frac{p_g^2}{M^2} G_{gN\bar{N}}^{(2)} \right), \quad (4.6)$$

and

$$\Gamma_-^g = \frac{-256}{35\sqrt{3}\mu^2 M^2} \frac{G_{gK\bar{K}} G_{gN\bar{N}}^{(1)}}{4\pi}, \quad (4.7)$$

where the latter are defined by the effective Lagrangian density

$$\begin{aligned} \mathcal{L} = & \left( \frac{4i}{\mu^2} G_{gK\bar{K}} \bar{K} \overset{\leftrightarrow}{\partial}_{\alpha\beta\gamma} \tau K + \frac{8}{M^2} G_{gN\bar{N}}^{(1)} \bar{N} \gamma_{\alpha} \partial_{\beta\gamma} \tau N \right. \\ & \left. + \frac{8i}{M^3} G_{gN\bar{N}}^{(2)} \partial_{\alpha} \bar{N} \tau \partial_{\beta\gamma} N \right) \cdot g^{\alpha\beta\gamma}, \end{aligned} \quad (4.8)$$

and the field notations follow [15,16]. Using (4.5) gives

$$G_{gN\bar{N}}^{(2)}/G_{gN\bar{N}}^{(1)} = 0.3 \pm 4.8, \quad (4.9)$$

the very large error being due to strong cancellations in (4.6) and (4.7). However, there is satisfactory agreement with the result  $-2.5 \pm 2.5$  obtained from  $\pi N$  analyses [3].

To estimate the  $gN\bar{N}$  couplings separately we first obtain  $G_{gK\bar{K}}$  from the decay  $g \rightarrow K\bar{K}$  via the width relation

$$\Gamma_{gK\bar{K}} = \frac{32q_g^7}{35\pi\mu^4 m_g^2} G_{gK\bar{K}}^2. \quad (4.10)$$

The  $g \rightarrow K\bar{K}$  branching ratio is poorly known the best estimate being [17,18] ( $1.5 \pm 0.5$ )%. This gives  $|G_{gK\bar{K}}| = 0.012 \pm 0.003$ , and leads to the estimates

$$\begin{aligned} G_{gN\bar{N}}^{(1)2}/4\pi &= 0.18 \pm 0.12, \\ |G_{gN\bar{N}}^{(1)} + 0.2G_{gN\bar{N}}^{(2)}| &= 1.7 \pm 1.0. \end{aligned}$$

The value of  $|G_{\omega N\bar{N}}^{(1)}|$  is far smaller than obtained in  $\pi N$  analyses [3], and may reflect the difficulty of extracting the very small  $g$ -contribution in the presence of a dominant  $\rho$ -term.

#### 4.2. $\omega$ , $\phi$ and $\omega^*$ Mesons

These contribute to  $D_3^+$  and  $D_1^-$ , and again only the two lowest spin states are necessary to obtain a satisfactory fit, although now there is the complication of two  $J=1$  resonances. Because of the relative closeness in mass of the two latter states, compared to their distance from the fitted region, it is not possible to effect a reliable separation of their contributions, and we therefore present results for a single pole placed at the mass of the  $\omega$ . Neglect of the  $\phi$  has some support from the validity of Zweig's rule [19], which predicts that the ideally mixed  $\phi$  decouples from  $NN$ . However, phenomenologically, this result is not exact, and so the  $\omega$  terms should be viewed as *effective* couplings, probably containing some effects of the  $\phi$  meson. The spin-3  $\omega^*$  (which itself could possibly be a mixture of two isospin states) is unambiguously present, both from its important role in achieving a fit to  $D_3^+$ , and the fact that the subtracted discrepancies show a marked  $a$ -dependence at fixed- $t$ . The fit to  $D_3^+$  and  $D_1^-/\nu$  using the  $BK$  amplitudes as the  $u$ -channel input are shown in Fig. 2.

The fitted values of the  $\omega$ -effective residues are

$$\Gamma_+^\omega = -1.6 \pm 0.3, \quad \Gamma_-^\omega = -3.0 \pm 0.4. \quad (4.11)$$

These are related to the  $\omega$  couplings of [13] by

$$\Gamma_+^\omega = \frac{-2M}{3} \frac{G_{\omega K\bar{K}}}{4\pi} \left( G_{\omega N\bar{N}}^{(V)} + \frac{m_\phi^2}{4M^2} G_{\omega N\bar{N}}^{(T)} \right), \quad (4.12)$$

and

$$\Gamma_-^\omega = \frac{-2\sqrt{2}}{3} \frac{G_{\omega K\bar{K}}}{4\pi} (G_{\omega N\bar{N}}^{(V)} + G_{\omega N\bar{N}}^{(T)}). \quad (4.13)$$

Using (4.10) gives

$$G_{\omega N\bar{N}}^{(T)}/G_{\omega N\bar{N}}^{(V)} = 0.4 \pm 0.7, \quad (4.14)$$

which is consistent with both the often made assumption [20] that  $G_{\omega N\bar{N}}^{(T)} \approx 0$  (which is supported by extrapolating Regge-pole fits of kaon-nucleon data [12]), and the value 0.69 found in a recent extensive fit to  $NN$  data using one-boson-exchange (OBE) potentials [21]. Individual values of  $G_{\omega K\bar{K}} G_{\omega N\bar{N}}^{(V)}$  follow from (4.13) and (4.14), and when averaged give

$$G_{\omega K\bar{K}} G_{\omega N\bar{N}}^{(V)}/4\pi = 2.3 \pm 0.7, \quad (4.15)$$

in excellent agreement with values in the region of 2.1 obtained from particle-exchange model fits to low-energy  $K^+p$  data [20], which also replaced the  $\omega$  and  $\phi$  by an effective- $\omega$  pole. If we *assume* that our results are dominantly due to the true  $\omega$ , then we can calculate  $G_{\omega N\bar{N}}$  using an estimate of  $G_{\omega K\bar{K}}$ . The latter may be obtained via the  $\phi \rightarrow K\bar{K}$  partial width

$$\Gamma_{\phi K\bar{K}} = \frac{4}{3} \frac{q_\phi^3}{m_\phi^2} \left( \frac{G_{\phi K\bar{K}}^2}{4\pi} \right),$$

and the  $SU(3)$  relation  $G_{\phi K\bar{K}} = -\sqrt{2} G_{\omega K\bar{K}}$ . Using a  $\phi \rightarrow K\bar{K}$  branching ratio of 0.84 yields

$$|G_{\omega K\bar{K}}| = 2.9 \pm 0.2,$$

and hence

$$G_{\omega N\bar{N}}^2/4\pi = 7.9 \pm 2.9, \quad (4.16)$$

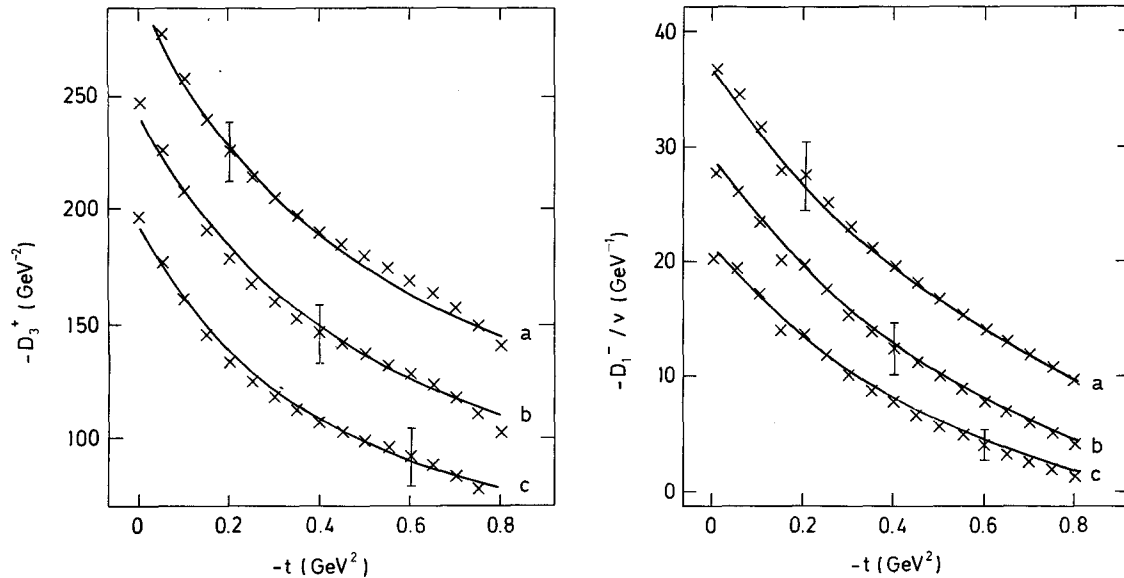
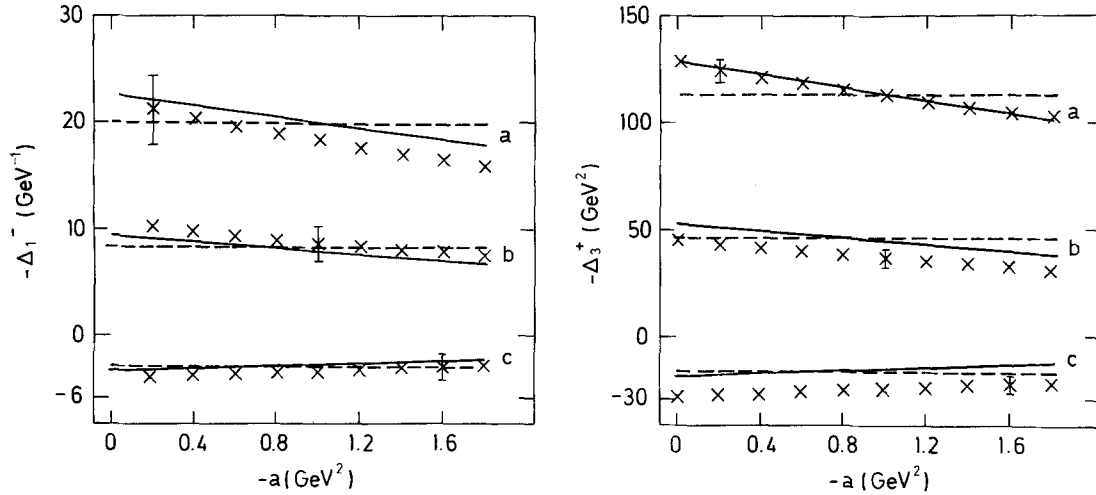


Fig. 2. Fit (—), using  $\omega$ -effective and  $\omega^*$  contributions, to the  $t$ -dependence of  $D_3^+$  and  $D_1^-/\nu(X)$ , for  $a=0$  (a),  $a=-0.6 \text{ GeV}^2$  (b) and  $a=-1.8 \text{ GeV}^2$  (c). Some typical error bars are shown



**Fig. 3.** Fits (—: including  $\omega^*$ , ---: excluding  $\omega^*$ ) to the  $a$ -dependence of  $A_1^-$  and  $A_3^+$  ( $X$ ), for  $t_1=0$  (a),  $t_1=-0.25$   $\text{GeV}^2$  (b) and  $t_1=-0.8$   $\text{GeV}^2$  (c), all subtracted at  $t_2=-0.6$   $\text{GeV}^2$ . Some typical error bars are shown

which is compatible with estimates from OBE fits to  $NN$  data [13].

The spin-3  $\omega^*$  is found to be necessary to produce an acceptable fit to the discrepancies. Moreover, the subtracted discrepancies show a significant  $a$ -dependence which is well approximated by a spin-3 contribution as is shown in Fig. 3. The values of the fitted residues are

$$\Gamma_{\omega^*}^{\omega^*} = -0.7 \pm 0.1, \Gamma_{\omega^*}^{\omega^-} = -0.9 \pm 0.2, \quad (4.17)$$

and are stable with respect to the inclusion or not of a separate  $\phi$  pole. The residues lead, via formulas analogous to (4.6) and (4.7) (identical except for an overall sign change), to the estimates

$$G_{\omega^* NN}^{(2)}/G_{\omega^* NN}^{(1)} = -0.2 \pm 1.3,$$

$$G_{\omega^* K\bar{K}} G_{\omega^* NN}^{(1)}/4\pi = (3.7 \pm 0.7)10^{-3}.$$

#### 4.3. $\delta$ and $A_2$ Mesons

The scalar  $\delta$  resonance contributes to  $D_2^+$  only, whereas the  $A_2$  contributes to both  $D_2^+$  and  $D_4^-$ . No higher spin states need be invoked, and the resulting fits are shown in Fig. 4. The dispersion relation evaluations show considerable noise, due largely to strong cancellations between terms. (Note that the errors shown are due solely to the range of hyperon couplings used). The effect of these cancellations is that in  $D_2^+$  the  $A_2$  contribution is found to dominate that of the  $\delta$ . The importance of the  $A_2$  can also be seen from the plot of  $A_2^+$  (Fig. 5) which exhibits a greater variation over  $a$  than the variation of the mean value (the dotted line, which is the  $\delta$  contribution) over  $t$ . Thus the situation is qualitatively different than that observed for the spin-3 mesons  $g$  and  $\omega^*$ , which were secondary effects. The curvature might

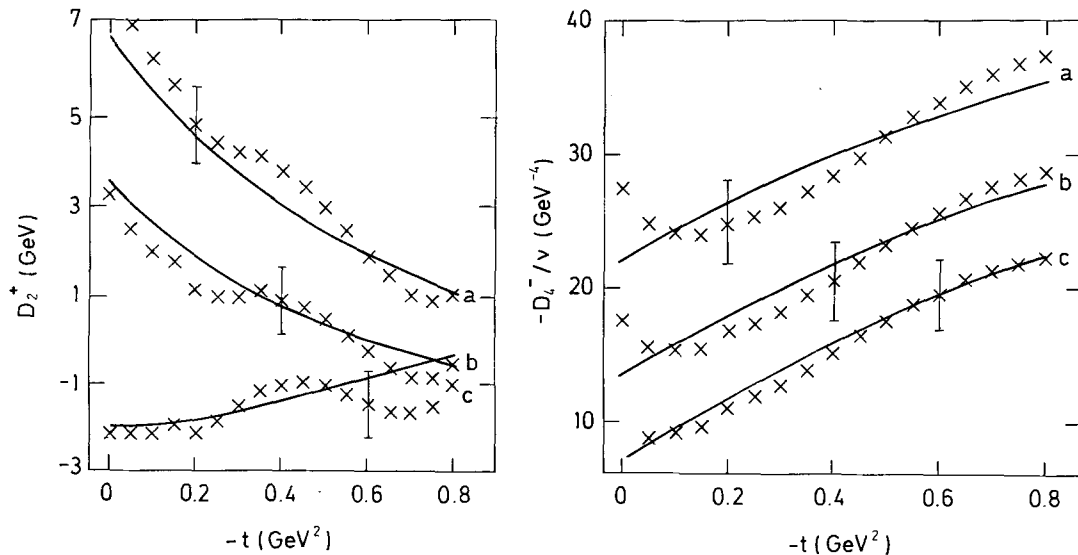


**Fig. 4.** Fit (—), using  $\delta$  and  $A_2$  contributions, to the  $t$ -dependence of  $D_2^+$  and  $D_4^-/v(X)$ , for  $a=0$  (a),  $a=-0.8$   $\text{GeV}^2$  (b) and  $a=-1.8$   $\text{GeV}^2$  (c). Some typical error bars are shown

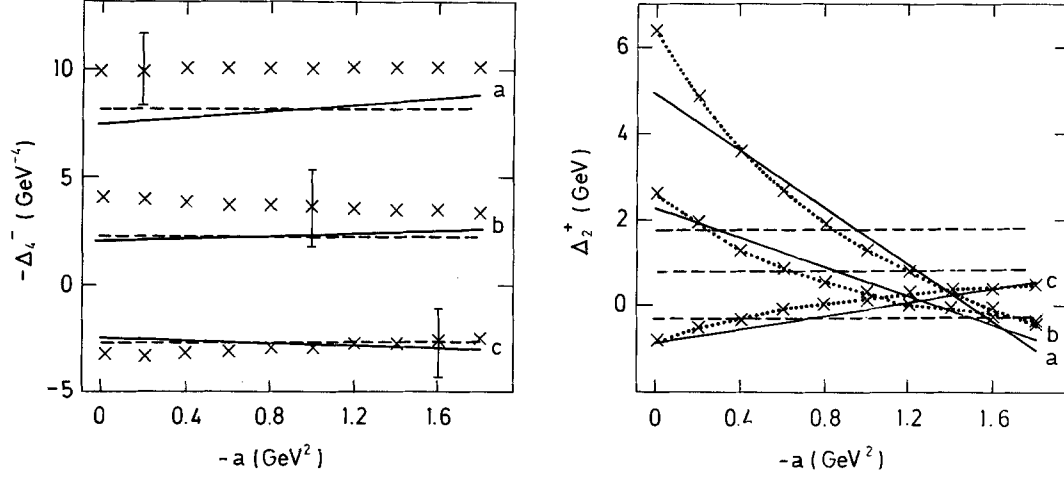


**Fig. 5.** Fits (---:  $\delta$  only,  $-\delta$  and  $A_2$ ) to the  $a$ -dependence of  $\Delta_4^-$  and  $\Delta_2^+(X)$  (shown joined by dots in the case of  $\Delta_2^+$ ), for  $t_1 = 0$  (a),  $t_1 = -0.25 \text{ GeV}^2$  (b),  $t_1 = -0.7 \text{ GeV}^2$  (c) in the case of  $\Delta_2^+$ , and  $t_1 = -0.15 \text{ GeV}^2$  (a),  $t_1 = -0.45 \text{ GeV}^2$  (b) and  $t_1 = -0.8 \text{ GeV}^2$  (c) in the case of  $\Delta_4^-$ , all subtracted at  $t_2 = -0.6 \text{ GeV}^2$ . Some typical error bars are shown

suggest the presence of a spin-4 contribution, but attempts to include such a term produce only marginally better fits, and a residue which is consistent with zero. The same is true for the  $\Delta_4^-$  discrepancy also shown in Fig. 5.

The fitted values of the residues are

$$\Gamma_+^\delta = 0.4 \pm 0.2, \quad (4.18)$$

$$\Gamma_+^{A_2} = 0.23 \pm 0.06, \quad \Gamma_-^{A_2} = -1.9 \pm 0.5, \quad (4.19)$$

and despite the poor quality of the fits, these are very stable to changes in the input data. Using the couplings of [13] gives

$$\Gamma_+^\delta = -\mu p_\delta^2 G_{\delta K\bar{K}} G_{\delta N\bar{N}}/4\pi,$$

which using (4.18) yields

$$G_{\delta K\bar{K}} G_{\delta N\bar{N}}/4\pi = 4.5 \pm 2.3, \quad (4.20)$$

The value of  $G_{\delta K\bar{K}}$  can in principle be found from the decay  $\delta \rightarrow K\bar{K}$  but the branching ratio is very poorly known. However, a recent analysis [22] of the decay properties of the  $\delta$  in the reactions  $K^- p \rightarrow \eta \pi^- \Sigma^*$  and  $K^- p \rightarrow K^0 K^- \Sigma^*$  has shown that the  $SU(3)$  prediction  $G_{\delta K\bar{K}}^2 = (3/2)G_{\delta\eta\pi}^2$  is well obeyed, and the latter may be obtained from

$$\Gamma_{\delta\eta\pi} = \frac{k\mu^2}{m_\delta^2} \frac{G_{\delta\eta\pi}^2}{4\pi},$$

where  $k$  is the  $\eta\pi$  c.m. momentum.

Using  $\Gamma_{\delta\eta\pi} = 50 \pm 10 \text{ MeV}$  [17] gives

$$|G_{\delta K\bar{K}}| = 9.8 \pm 1.0,$$

and from (4.20)

$$G_{\delta N\bar{N}}^2/4\pi = 2.6 \pm 3.2 \quad (4.21)$$

which is also in good agreement with  $NN$  analyses [13, 21].

For the  $A_2$  residues we have

$$\Gamma_+^{A_2} = \frac{32}{15\mu} \frac{G_{A_2 K\bar{K}}}{4\pi} \left( G_{A_2 N\bar{N}}^{(1)} - \frac{p_{A_2}^2}{M^2} G_{A_2 N\bar{N}}^{(2)} \right), \quad (4.23)$$

and

$$\Gamma_-^{A_2} = \frac{16\sqrt{6}}{15\mu M} \frac{G_{A_2 K\bar{K}} G_{A_2 N\bar{N}}^{(1)}}{4\pi}, \quad (4.23)$$

which using (4.19) give

$$G_{A_2 N\bar{N}}^{(2)}/G_{A_2 N\bar{N}}^{(1)} = -2.3 \pm 0.2, \quad (4.24)$$

and

$$G_{A_2 K\bar{K}} G_{A_2 N\bar{N}}^{(1)}/4\pi = -0.09 \pm 0.02. \quad (4.25)$$

Finally,  $|G_{A_2 K\bar{K}}|$  may be obtained from the decay  $A_2 \rightarrow K\bar{K}$  via

$$\Gamma_{A_2 K\bar{K}} = \frac{8q_{A_2}^5}{15\pi\mu^2 M_{A_2}^2} G_{A_2 K\bar{K}}^2.$$

Using a branching ratio of  $(4.7 \pm 0.5)\%$  [17] gives  $|G_{A_2 K\bar{K}}| = 0.25 \pm 0.02$  and hence

$$G_{A_2 N\bar{N}}^{(1)2}/4\pi = 1.6 \pm 0.9. \quad (4.26)$$

#### 4.4. $f$ and $f'$ Mesons

These contribute to  $D_1^+$  and  $D_3^-$ . The former also has a scalar contribution, which presents special problems, and we defer discussion of this to Sect. 4.5. As in the  $\omega - \phi$  case the relative closeness in mass of the  $f$  and  $f'$  with respect to their distance from the fitting region precludes the use of two distinct poles. The fit to  $D_3^-$  using a single effective pole at the  $f$  mass is shown in Fig. 6, and the resulting value of the residue is

$$\Gamma_- = 6.5 \pm 0.3 \quad (4.27)$$



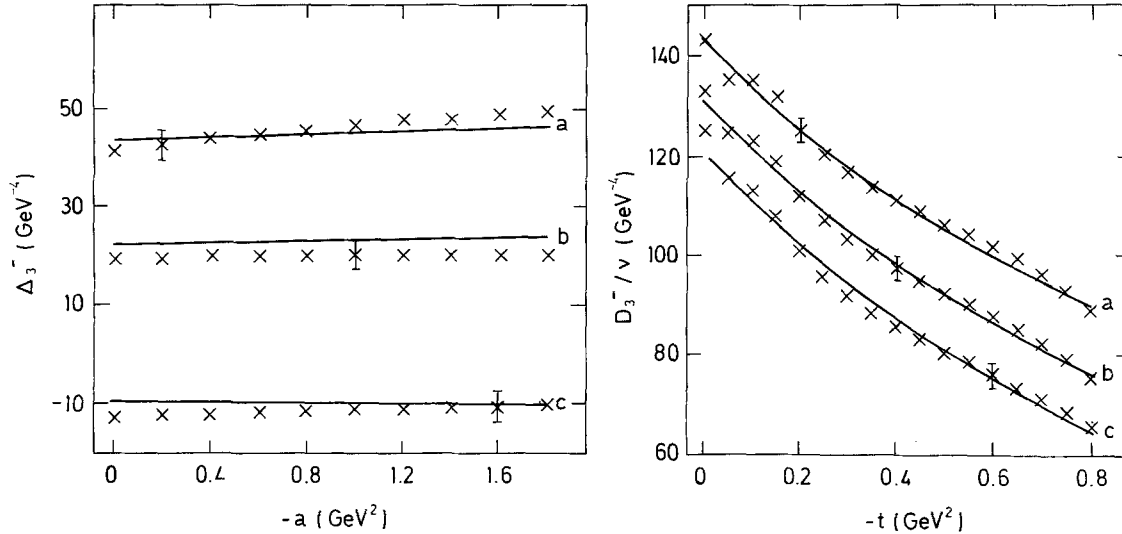


**Fig. 6.** Fit (—), using a single  $f$ -effective pole, to the  $t$ -dependence of  $D_3^-/\nu(X)$ , for  $a=0$  (a),  $a=-0.8$  GeV<sup>2</sup> (b) and  $a=-1.8$  GeV<sup>2</sup> (c); and to the  $a$ -dependence of  $\Delta_3^-(X)$ , for  $t_1=0$  (a),  $t_1=-0.45$  GeV<sup>2</sup> (b) and  $t_1=-0.8$  GeV<sup>2</sup> (c), all subtracted at  $t_2=-0.6$  GeV<sup>2</sup>. Some typical error bars are shown

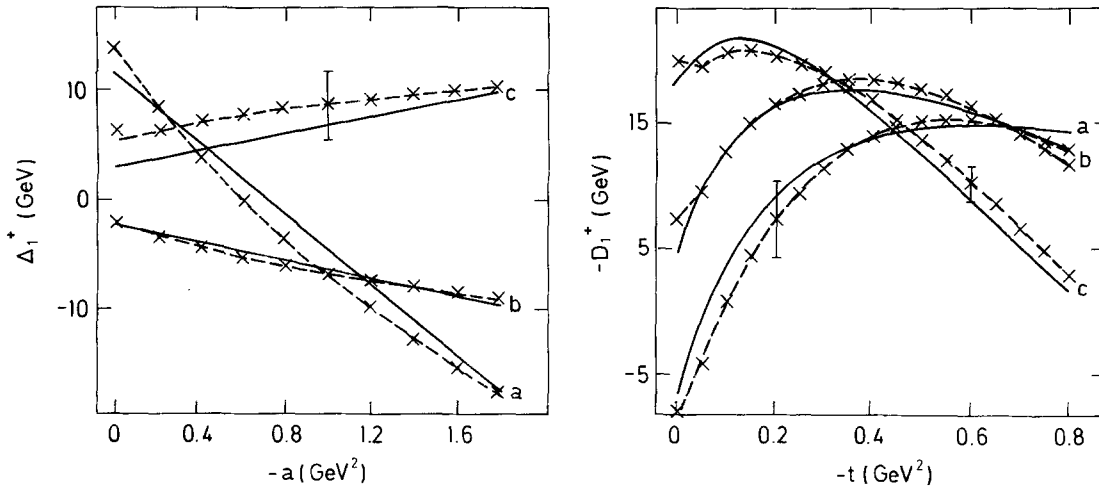


**Fig. 7.** Fit (—), using scalar and  $f$ -effective contributions, to the  $t$ -dependence of  $D_1^+(X)$ , for  $a=0$  (a),  $a=-0.6$  GeV<sup>2</sup> (b) and  $a=-1.8$  GeV<sup>2</sup> (c); and to the  $a$ -dependence of  $\Delta_1^+(X)$ , for  $t_1=0$  (a),  $t_1=-0.4$  GeV<sup>2</sup> (b), and  $t_1=-0.8$  GeV<sup>2</sup>, all subtracted at  $t_2=-0.6$  GeV<sup>2</sup>. Some typical error bars are shown

Inclusion of a  $J=4$  term (the  $h$ -meson) produces no significant improvement in the fit, and a residue which is consistent with zero. The absence of a significant  $h$  contribution is confirmed by the lack of substantial  $a$ -dependence in  $\Delta_3^-$  (Fig. 6). The fit to  $D_1^+$  with  $f$ -effective and scalar contributions will be described later, but the resulting residue

$$\Gamma_+ = 1.3 \pm 0.2, \quad (4.28)$$

is very insensitive to the form of the scalar term, even though the latter contribution is substantial. This situation is analogous to the  $g$  and  $\omega^*$  cases where dominance of the lower spin effects with regard to the  $t$ -dependence stabilises the values of the higher spin

residues. The importance of a  $J=2$  contribution can be seen from the strong  $a$ -dependence of  $\Delta_1^+$  shown in Fig. 7.

Detailed interpretation of  $\Gamma_\pm$  is difficult because, unlike in the  $\pi N$  case, Zweig's rule does not lead to a strong suppression of the  $f'$  with respect to the  $f$ . Thus we have no reason to neglect either the  $f$  or the  $f'$  contribution. However, we can make rough estimates of the relative strength of these two terms. To do this we write

$$\Gamma_\pm \approx \Gamma_\pm^f + \left\langle \frac{m_f^2 - t}{m_{f'}^2 - t} \right\rangle \Gamma_\pm^{f'},$$

where  $\langle \dots \rangle = 0.75$  is an average over the range of

the fit. In terms of  $f$  and  $f'$  couplings,

$$\Gamma_+ \approx \frac{32}{15\mu} \left[ \frac{G_{fK\bar{K}}}{4\pi} \left( G_{fN\bar{N}}^{(1)} - \frac{p_f^2}{M^2} G_{fN\bar{N}}^{(2)} \right) + 0.75 \frac{G_{f'K\bar{K}}}{4\pi} \left( G_{f'N\bar{N}}^{(1)} - \frac{p_{f'}^2}{M^2} G_{f'N\bar{N}}^{(2)} \right) \right], \quad (4.29)$$

and

$$\Gamma_- \approx \frac{16\sqrt{6}}{15\mu M} \left( \frac{G_{fK\bar{K}} G_{fN\bar{N}}^{(1)}}{4\pi} + 0.75 \frac{G_{f'K\bar{K}} G_{f'N\bar{N}}^{(1)}}{4\pi} \right). \quad (4.30)$$

The moduli of  $G_{fK\bar{K}}$  and  $G_{f'K\bar{K}}$  may be obtained from the partial widths

$$\Gamma_{fK\bar{K}} = \frac{8q_s^5}{15\pi\mu^2 m_f^2} G_{fK\bar{K}}^2,$$

(similarly for  $f' \rightarrow K\bar{K}$ ), and their relative signs from  $SU(3)$ , assuming ideal mixing and the absence of  $f' \rightarrow \pi\pi$  decay (Zweig's rule) [19]. (We use  $K\bar{K}$  branching ratios of  $(3.1 \pm 0.4)\%$  and  $(90 \pm 10)\%$ , for  $f$  and  $f'$  decays, respectively). Also, from analyses of  $\pi N$  scattering [13] it is known that  $G_{fN\bar{N}}^{(2)} \approx 0$  and  $G_{fN\bar{N}}^{(1)} = 6.3 \pm 1.0$  (assuming, for definiteness,  $G_{f\pi\pi} > 0$ ). Collecting these results together, and using (4.29)–(4.30) yields the estimates

$$\frac{G_{f'K\bar{K}} G_{f'N\bar{N}}^{(1)}}{4\pi} \approx 0.2 \pm 0.1, \quad \frac{G_{fK\bar{K}} G_{fN\bar{N}}^{(2)}}{4\pi} \approx -0.8 \pm 0.5,$$

compared with

$$\frac{G_{fK\bar{K}} G_{fN\bar{N}}^{(1)}}{4\pi} = 0.16 \pm 0.04, \quad \frac{G_{f'K\bar{K}} G_{f'N\bar{N}}^{(2)}}{4\pi} \approx 0.$$

Thus the  $f'$  provides a very important contribution to the  $t$ -channel of  $KN$  scattering.

#### 4.5. Scalar Mesons

(a)  $\varepsilon, S^*$  Residues. The scalar mesons contribute to  $D_1^+$  along with the  $f$  and  $f'$ , but although the latter give important  $a$ -dependent terms (see Sect. 4.4), because of their relatively high masses they contribute only slightly to the  $t$ -dependence, which is dominated by the  $J=0$  amplitude. This function is shown in Fig. 7, and is qualitatively different from previous discrepancies in being distinctly non pole-like. To achieve the observed shape in a pole model with an essentially  $t$ -dependent background requires at least two nearby poles contributing with opposite signs. It is tempting to ascribe this behaviour to an interference between the  $\varepsilon$  and  $S^*$  mesons, but there is a difficulty because an acceptable fit can only be achieved with  $m_\varepsilon \approx 0.7$  GeV, whereas the physical  $\varepsilon$  has a mass  $\approx 1.3$  GeV. [17]. The narrow-width approximation is clearly inadequate, but fortunately it is possible to do better because detailed analyses of  $\pi N$  scattering [23] have deduced the form of the  $I=J=0$   $\pi\pi \rightarrow N\bar{N}$  helicity amplitude  $f_+^0(t)$  for  $\sqrt{t} \lesssim 0.9$  GeV. In particular  $\text{Im } f_+^0(t)$  is known to

have a broad maximum at  $\approx 0.7$  GeV, probably followed by a zero around 1 GeV. In a pole model the latter is interpreted [4] as the start of the  $S^*$  effect. Since  $m_\varepsilon \approx 1.3$  GeV we are led to a picture of  $\text{Im } f_+^0(t)$  as having a broad maximum due to the  $\varepsilon$ -meson “interrupted” by a negative minimum due to the  $S^*$ . A discrepancy analysis of  $\pi N$  scattering along the lines of the present work [4] lends support to this view. Beyond 1 GeV  $\text{Im } f_+^0(t)$  is essentially unknown, but destructive interference between the negative tail of the  $S^*$  and the positive  $\varepsilon$  would tend to occur. Thus the bulk of the  $\varepsilon$  contribution would arise from relatively low masses, and in a pole model would require a low effective mass for the  $\varepsilon$ , as has been found. Unfortunately, in this case the interpretation of the resulting residues is far from clear.

Fortunately, the  $t$ -dependence of  $D_1^+$  is not sensitive to the higher energy region of the helicity amplitudes, so we seek a way of inserting the low- $t$  behaviour of the scalar term without explicitly assuming a pole behaviour. We do this by assuming that the qualitative behaviour of  $h_+^0(t)$  in this region is similar to that of  $f_+^0(t)$ , i.e. we assume that

$$\text{Im } h_+^0(t) = 2R_\varepsilon \text{Im } f_+^0(t), \quad (4.31)$$

for  $\sqrt{t} \lesssim 0.9$  GeV, and we interpret  $R_\varepsilon$  as the ratio of  $\varepsilon$  couplings to  $K\bar{K}$  and  $\pi\pi$ . (The factor of two is a consequence of our definitions of couplings). This ansatz has been used before [20] in an analysis of  $K^+ p$  data, and some support for it comes from considering the unitarity condition, which in this region is well approximated by the  $\pi\pi$  intermediate state, and takes the form

$$\text{Im } h_+^0(t) = \frac{-3}{16\pi} \left[ \frac{t-4\mu^2}{4t} \right]^{1/2} [f_+^0(t)]^* g_0(t),$$

where  $g_0(t)$  is the  $J=0$  partial-wave amplitude for  $\pi\pi \rightarrow K\bar{K}$  [13]. Since the imaginary parts of both  $f_+^0$  and  $g_0$  are numerically far larger than their real parts [14, 23, 24], and  $\text{Im } g_0 < 0$  for  $\sqrt{t} < 0.9$  GeV [14, 24], equation (4.31) is a reasonable approximation with  $R_\varepsilon > 0$ . We retain the narrow-width form for the  $S^*$  resonance.

The fit to  $D_1^+$  is shown in Fig. 7, and the resulting parameters are

$$R_\varepsilon \equiv \frac{G_{\varepsilon K\bar{K}}}{G_{\varepsilon\pi\pi}} = 0.41 \pm 0.07, \quad (4.32)$$

and

$$\Gamma_+^{S^*} = -\mu p_{S^*}^2 \frac{G_{S^*K\bar{K}} G_{S^*N\bar{N}}}{4\pi} = -2.9 \pm 0.8, \quad (4.33)$$

where the errors reflect the use of different inputs for  $\text{Im } f_+^0$  [23] as well as  $u$ -channel amplitudes.

(b) *Scalar Nonet*. An  $SU(3)$  analysis of the scalar nonet is fraught with difficulties, not least of which

is to identify which states comprise the multiplet. We make the usual assumption [25] that the  $I = 0$  members are the  $\varepsilon$  and  $S^*$  mesons, with the  $\delta(980)$  as the  $I = 1$  component, although other assignments are certainly possible [26].

The singlet ( $g_1$ ) and octet ( $g_8$ ) couplings are defined via the  $SU(3)$  Lagrangian density

$$\mathcal{L}/\mu = g_1 \varepsilon_1 (\pi \cdot \pi + 2K\bar{K}) + g_8 [2\delta \cdot \pi \eta + \delta \cdot \bar{K} \tau K + S_8 (\pi \cdot \pi - \bar{K} K)],$$

and the  $\varepsilon - S^*$  mixing angle is defined by

$$\varepsilon = \varepsilon_1 \cos \theta - S_8 \sin \theta,$$

$$S^* = \varepsilon_1 \sin \theta + S_8 \cos \theta,$$

Then,

$$G_{\varepsilon\pi\pi} = 2g_1 \cos \theta - 2g_8 \sin \theta, \quad (4.34a)$$

$$G_{\varepsilon K\bar{K}} = 2g_1 \cos \theta + g_8 \sin \theta, \quad (4.34b)$$

$$G_{S^*\pi\pi} = 2g_1 \sin \theta + 2g_8 \cos \theta, \quad (4.34c)$$

$$G_{S^*K\bar{K}} = 2g_1 \sin \theta - g_8 \cos \theta, \quad (4.34d)$$

and in terms of these couplings the partial widths given by

$$\Gamma_{\varepsilon\pi\pi} = \frac{3k_\pi \mu^2 G_{\varepsilon\pi\pi}^2}{4m_\varepsilon^2 4\pi}, \quad \Gamma_{\varepsilon K\bar{K}} = \frac{k_K \mu^2 G_{\varepsilon K\bar{K}}^2}{m_\varepsilon^2 4\pi}, \quad (4.35)$$

where  $k_\pi, k_K$  are the appropriate c.m. momenta. Equations (4.34a, b) may be written

$$G_{\varepsilon K\bar{K}} = R_\varepsilon G_{\varepsilon\pi\pi} = -3R_\varepsilon g_8 \sin \theta / (1 - R_\varepsilon),$$

and using these in equation (4.35), plus the unitarity constraint

$$\Gamma_{\varepsilon\pi\pi} + \Gamma_{\varepsilon K\bar{K}} \leq \Gamma_\varepsilon \quad (4.36)$$

the total width, leads to the upper bound

$$\sin^2 \theta \leq \frac{4\pi m_\varepsilon^2 \Gamma_\varepsilon (1 - R_\varepsilon)^2}{9\mu^2 g_8^2 (\frac{3}{4}k_\pi + k_K R_\varepsilon^2)}. \quad (4.37)$$

A similar bound for  $\cos^2 \theta$  may be obtained in terms of  $R_{S^*} \equiv G_{S^*K\bar{K}}/G_{S^*\pi\pi}$ , but the precise value of this ratio is unknown. However, there is strong evidence that  $R_{S^*} > 0$ . This follows from combining the sign of  $\Gamma_{S^*+}$  in equation (4.33) with the results of a discrepancy analysis of  $\pi N$  amplitudes [4], and is supported by consideration of the qualitative features of the Legendre coefficients for  $K^+ K^-$  production in  $\pi N$  reactions [25]. An assumed positive value of  $R_{S^*}$  was in fact the basis of the  $SU(3)$  analysis of Morgan [25] which found a large mixing angle  $\theta \approx 69^\circ$ , but in Morgan's solution the  $\varepsilon$  is essentially decoupled from  $K\bar{K}$ , in contrast with more recent data [27]. Using (4.34)  $R_{S^*}$  may be written

$$R_{S^*} = \frac{\tan^2 \theta (1 + 2R_\varepsilon) + (1 - R_\varepsilon)}{\tan^2 \theta (1 + 2R_\varepsilon) - 2(1 - R_\varepsilon)},$$

and for  $0 < R_\varepsilon < 1, R_{S^*} > 0$  implies the lower bound

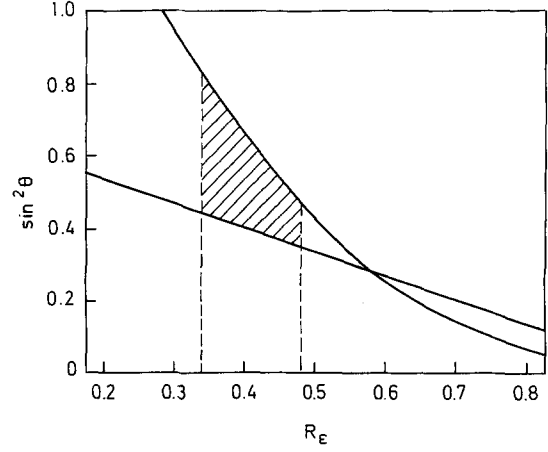


Fig. 8. Upper and lower bounds on  $\sin^2 \theta$  as a function of  $R_\varepsilon$ . The shaded region denotes the allowed  $(R_\varepsilon, \sin^2 \theta)$  domain

$$\sin^2 \theta \geq \frac{2}{3}(1 - R_\varepsilon). \quad (4.38)$$

The bounds (4.37) and (4.38) are plotted in Fig. 8 as a function of  $R_\varepsilon$ . To evaluate the upper bound we use  $m_\varepsilon = 1.3$  GeV,  $\Gamma_\varepsilon < 0.4$  GeV [17] and  $g_8^2 = 48.4$  as calculated from

$$\Gamma_{\delta\pi\pi} = \frac{2k\mu^2 g_8^2}{m_\delta^2 4\pi},$$

using a partial width of 50 MeV [22]. The shaded areas on Fig. 8 denotes the allowed regions for  $R_\varepsilon$  and  $\sin^2 \theta$ , from which we deduce our best value of  $\sin^2 \theta = 0.52 \pm 0.12$ . From  $R_\varepsilon$  and  $\sin^2 \theta$  we find  $|g_1/g_8| = 1.6 \pm 0.5$ , which is compatible with  $\sqrt{2}$ , the prediction of Zweig's rule [19]. All other couplings may now be calculated. For definiteness we use  $g_8^2 = 48.4$ , as before. For the  $\varepsilon$  we find

$$G_{\varepsilon\pi\pi}^2/4\pi = 52, \quad G_{\varepsilon K\bar{K}}^2/4\pi = 9,$$

which imply appreciable coupling to both  $\pi\pi$  and  $K\bar{K}$  channels ( $\Gamma_{\varepsilon\pi\pi} = 286$  MeV,  $\Gamma_{\varepsilon K\bar{K}} = 43$  MeV,  $\Gamma_\varepsilon \geq 329$  MeV) in agreement with recent production data [27]. For the  $S^*$ ,  $R_{S^*} = 3.4 \pm 2.2$  and

$$G_{S^*\pi\pi}/4\pi = 3, \quad G_{S^*K\bar{K}}^2/4\pi = 34, \quad (4.40)$$

which imply a satisfactory small  $S^* \rightarrow \pi\pi$  width of 23 MeV. The  $S^* \rightarrow K\bar{K}$  width depends critically on the mass of the  $S^*$  because of the phase-space factor, but for  $M_{S^*} < 1$  GeV,  $\Gamma_{S^*K\bar{K}} < 50$  MeV and so  $23 < \Gamma_{S^*} < 73$  MeV, again in good agreement with experiment [17]. Finally, using (4.40) in (4.33) gives  $G_{S^*NN}^2/4\pi = 31$ .

Although the above analysis leads to results in excellent agreement with experiment, it is worth remarking that the  $\varepsilon$  and  $S^*$  couplings depend on  $g_8^2$ , which we have calculated from  $\delta \rightarrow \pi\eta$  decay. However, the same coupling can be obtained from  $\kappa \rightarrow K\pi$ , and although the parameters of this decay are not precisely known, current estimates imply a considerably larger value for  $g_8^2$  and a consequent increase in the  $\varepsilon$  and  $S^*$  partial widths.

## References

1. Pietarinen, E. : Helsinki preprint 1978, and 'Proceedings of the Topical Conference on Baryon Resonances', Oxford 1976; Devenish, R.C.E., Froggatt, C.D., Martin, B.R. : Nucl. Phys. **B81**, 330 (1974)
2. Groom, M.S., Martin, B.R. : Nucl. Phys. **B97**, 36 (1975); Contogouris, A.P., Svec, M. : Phys. Rev. **D17**, 806 (1978)
3. Jacob, R., Hite, G.E. : Phys. Rev. **D11**, 2466 (1975); Kaiser, F., Borie, E., Hohler, G. : Phys. Lett. **62B**, 441 (1976); Borie, E., Kaiser, F. : Nucl. Phys. **B126**, 173 (1977)
4. Hedegaard-Jensen, N. : Nucl. Phys. **B119**, 27 (1977)
5. Martin, B.R. : Springer Tracts in Modern Physics **55**, 73 (1970)
6. Hite, G.E., Steiner, F. : CERN TH1590 (1972); Nuovo Cimento **18A**, 237 (1973)
7. Martin, B.R. : Nucl. Phys. **B94**, 413 (1975)
8. Alson-Garnjost, M., Kenny, R.W., Pollard, D.L., Ross, R.R., Tripp, R.D., Nicholson, H., Ferro-Luzzi, M. : Phys. Rev. **D18**, 182 (1978)
9. Gopal, G.P., Ross, R.T., Van Horn, A.J., McPherson, A.C., Clayton, E.F., Bacon, T.C., Butterworth, I. : Nucl. Phys. **B119**, 362 (1977)
10. Martin B.R., Pidcock, M.K. : Nucl. Phys. **B126**, 266, 285 (1977)
11. Martin, A.D. : Phys. Lett. **65B**, 346 (1976)
12. Joynton, D.W., Martin, B.R. : Nucl. Phys. **B134**, 83 (1978)
13. Nagels, M.M., De Swart, J.J., Neilsen, H., Oades, G.C., Petersen, J.L., Tromberg, B., Gustafson, G., Irving, A.C., Jarlskog, C., Pfeil, W., Pilkuhn, H., Steiner, F., Tauscher, L. : Nucl. Phys. **B109**, 1 (1976)
14. Hedegaard-Jensen, N. : Nucl. Phys. **B77**, 173 (1974)
15. Bjorken, J.D., Drell, S.D. : 'Relativistic Quantum Fields', New York: McGraw-Hill 1965
16. Carruthers, P.A., 'Spin and Isospin in Particle Physics', London, New York: John Wiley
17. Particle Data Group, Phys. Lett **75B**, 1 (1978)
18. Martin, A.D., Ozmutlu, E.N., Baldi, R., Böhringer, T., Dorsaz, P.A., Hungerbühler, V., Kienzle-Focacci, N.N., Martin, M., Mermoud, A., Nef, C., Siegrist, P. : Nucl. Phys. **B140**, 158 (1978)
19. Zweig, G. : CERN preprints TH401, 402; Okubo, S. : Phys. Lett. **5**, 105 (1963); Iizuka, J., Okada, K., Shito, O. : Prog. Theor. Phys. **35**, 1061 (1963);
20. Alcock, J.W., Cottingham, W.N., Davies, A.C. : Nucl. Phys. **B102**, 173 (1976)
21. Rijken, T.A., Nagels, M.M., DeSwart, J.J. : quoted in Ref. [13]; Nagels, M.M., Rijken, T.A., De Swart, J.J. : Phys. Rev. **D12**, 744 (1975)
22. Irving, A.C. : Phys. Lett. **70B**, 217 (1977)
23. Gustafson, G., Neilsen, H., Oades, G.C. : Aarhus report (1975); Peitarinen, E. : Helsinki report (1975), both quoted in Ref. [13]
24. Johannesson, N.O., Petersen, J.L. : Nucl. Phys. **B68**, 397 (1973)
25. Morgan, D. : Phys. Lett. **51B**, 71 (1974)
26. Martin, B.R., Reinders, L.J. : Nucl. Phys. **B143**, 309 (1978)
27. Pawlicki, A.J., Ayres, D.S., Cohen, D., Diebold, R., Kramer, S.L., Wicklund, A.B. : Phys. Rev. Lett. **39**, 971 (1976)

Received 28 November 1978